Molecules and Cells

Characterization of *TNNC1* as a Novel Tumor Suppressor of Lung Adenocarcinoma

Suyeon Kim[1,2,5], Jaewon Kim[1,2,5], Yeonjoo Jung[1,2,5], Yukyung Jun[1,2], Yeonhwa Jung[2], Hee-Young Lee[2], Juhee Keum[2], Byung Jo Park[3], Jinseon Lee[4], Jhingook Kim[3], Sanghyuk Lee[1,2,*], and Jaesang Kim[1,2,*]

[1]Department of Life Science, Ewha Womans University, Seoul 03760, Korea, [2]Ewha Research Center for Systems Biology, Ewha Womans University, Seoul 03760, Korea, [3]Department of Thoracic and Cardiovascular Surgery, Samsung Medical Center, Sungkyunkwan University School of Medicine, Seoul 06351, Korea, [4]Samsung Biomedical Research Institute, Samsung Medical Center, Sungkyunkwan University School of Medicine, Seoul 06351, Korea, [5]These authors contributed equally to this work.
*Correspondence: sanghyuk@ewha.ac.kr (SL); jkim1964@ewha.ac.kr (JK)
https://doi.org/10.14348/molcells.2020.0075
www.molcells.org

In this study, we describe a novel function of *TNNC1* (Troponin C1, Slow Skeletal and Cardiac Type), a component of actin-bound troponin, as a tumor suppressor of lung adenocarcinoma (LUAD). First, the expression of *TNNC1* was strongly down-regulated in cancer tissues compared to matched normal lung tissues, and down-regulation of *TNNC1* was shown to be strongly correlated with increased mortality among LUAD patients. Interestingly, *TNNC1* expression was enhanced by suppression of *KRAS*, and ectopic expression of *TNNC1* in turn inhibited *KRAS*^{G12D}-mediated anchorage independent growth of NIH3T3 cells. Consistently, activation of KRAS pathway in LUAD patients was shown to be strongly correlated with down-regulation of *TNNC1*. In addition, ectopic expression of *TNNC1* inhibited colony formation of multiple LUAD cell lines and induced DNA damage, cell cycle arrest and ultimately apoptosis. We further examined potential correlations between expression levels of *TNNC1* and various clinical parameters and found that low-level expression is significantly associated with invasiveness of the tumor. Indeed, RNA interference-mediated down-regulation of *TNNC1* led to significant enhancement of invasiveness *in vitro*. Collectively, our data indicate that *TNNC1* has a novel function as a tumor suppressor and is targeted for down-regulation by KRAS pathway during the carcinogenesis of LUAD.

Keywords: invasion, *KRAS*, lung adenocarcinoma, *TNNC1*, tumor suppressor

INTRODUCTION

Lung cancer represents one of the top-ranked cancers in terms of both incidence and mortality (Siegel et al., 2018). In United States, 234,030 new cases of lung and bronchus cancer had been predicted to occur in 2018 which in terms of incidence would represent the second highest among all types of cancer (Siegel et al., 2018). Approximately 83,550 men and 70,500 women were projected to die that year from this disease which has been the leading cause of cancer-related death for over 25 years (Siegel et al., 2018). Given the poor prospect with the overall five-year survival rate of less than 20%, there is an urgent need for development of new diagnostic and therapeutic strategies (Siegel et al., 2018).

The most significant contribution to this end is likely to come from large-scale high-throughput sequencing projects and systems biological analyses which have provided comprehensive molecular profiling of multiple types of cancer. For lung cancers, the most notable study was published in 2014 by The Cancer Genome Atlas Research Network, a genomics program aiming to molecularly characterize primary cancers

Received 20 March, 2020; revised 13 April, 2020; accepted 17 April, 2020; published online 8 July, 2020

eISSN: 0219-1032

and matched normal samples of multiple cancer types (Cancer Genome Atlas Research Network, 2014). This particular study used 230 resected surgical samples whose transcriptome and exome were subsequently profiled for somatic mutations, differentially expressed genes (DEGs) and altered pathways. Data from such studies are expected to bring new understanding to carcinogenesis at the molecular level and point to candidate actionable events. However, given that large scale studies typically result in hundreds of mutations and thousands of DEGs, there is a great need to distinguish the so-called drivers and passengers among mutations and DEGs based on functional analyses.

Troponin, a complex of three regulatory proteins Troponin C, Troponin I and Troponin T, is best known for regulating muscle contraction as a component of the thin filament (Johnston et al., 2018). Accordingly, they are abundantly expressed in cytoplasm of skeletal and cardiac muscle cells. Mounting evidence also suggests that various subunits of troponin are expressed in non-muscle tissues and cells. These include eye, brain, ovary, lung, bone, and liver (Berezowsky and Bag, 1992; Chen et al., 2014; Johnston et al., 2018; Leung et al., 2014; Moses et al., 1999; Schmidt et al., 2006). Interestingly, some of the troponin genes are found in nucleus rather than cytoplasm depending on cell types and were proposed to be involved in nuclear processes including transcription by RNA polymerase II (Casas-Tinto et al., 2016; Chase et al., 2013; Johnston et al., 2018; Sahota et al., 2009). Most intriguingly, troponin genes are expressed in diverse cancer cells and in immortalized cell lines and show oncogenic or tumor suppressor activities. For example, slow skeletal and cardiac type Troponin C1 (*TNNC1*) has been shown to mediate oncogenic activity of microfibrillar-associated protein 5 (MFAP5) in ovarian cancer cells (Leung et al., 2014). Slow skeletal type Troponin I1 (*TNNI1*) is also reported to possess oncogenic activity as its down-regulation inhibited proliferation of human non-small cell lung carcinoma xenografts in mice (Casas-Tinto et al., 2016). In contrast, fast skeletal type Troponin I2 (TNNI2) has been reported to contain a potent inhibitory effect on blood vessel formation and thereby lead to inhibition of tumor growth (Moses et al., 1999).

Here, we present data indicating that *TNNC1* functions as a tumor suppressor of lung adenocarcinoma (LUAD). *TNNC1* is shown to be a DEG whose down-regulated expression is closely associated with KRAS activity and with poor survival. We present evidence from molecular functional analyses indicating that TNNC1 mediates cell cycle regulation, apoptosis and tumor invasion as well.

MATERIALS AND METHODS

Patient samples and transcriptome analyses

Tumor and normal tissue samples were obtained from patients who had undergone curative surgery at the Samsung Medical Center (Korea). Informed consents were obtained from patients, and all plans and procedures were approved by the Institutional Review Boards of Samsung Medical Center (IRB No. 2010-08-063-006) in accordance with the Declaration of Helsinki. RNAseq for the said samples has been described (Yu et al., 2019), and the data for the tumor and matched normal samples were processed according to the TCGA pipeline of MapSplice-RSEM (Li and Dewey, 2011; Wang et al., 2010) using Ensembl 81 genome and transcript models. Sequence reads were normalized within-samples to the upper quartile of total reads. DEGs were obtained using Voom (Law et al., 2014) with false discovery rate < 0.001. TCGA gene expression data were downloaded at level 3 from the Broad GDAC Firehose website (released on January 28, 2016) (Cerami et al., 2012; Gao et al., 2013).

KRAS pathway activity analysis

The Hallmark gene sets and C2 gene sets from the molecular signature database (MSigDB) were used to examine the correlation between the expression level of *TNNC1* and the activity of KRAS pathway. Tumor RNA-Seq data from 502 LUAD patients were used in the analysis. The pathway activity score was calculated using the GSVA method in R package. The *TNNC1* expression levels for each group were compared by two sided Student's *t*-test.

Cell culture

A549 and NCI-H2009, human LUAD cell lines, were obtained from the American Type Culture Collection (ATCC, USA). Cells were cultured in RPMI-1640 supplemented with 10% fetal bovine serum (Hyclone, USA). NIH3T3, mouse embryonic fibroblast cells were purchased from the ATCC and cultured in DMEM supplemented with 10% calf serum (Invitrogen, USA).

Knockdown of *KRAS* and real-time PCR analysis

A549 or H2009 cells at 40% confluence were transfected with 40 nM *KRAS* siRNA using Lipofectamine RNAiMAX (Invitrogen). siRNA duplexes of *KRAS* and scrambled negative control (NC) were obtained from Qiagen (USA). The target sequences of *KRAS* siRNAs are listed in Supplementary Table S1. After 48 h, total RNA was extracted using the TRIzol reagent (Invitrogen), and cDNA was synthesized by using GoScirpt reverse transcriptase (Promega, USA) according to the manufacturer's instructions. Real-time polymerase chain reaction (PCR) analysis was carried out using CFX96 Real-time PCR detection system (Bio-Rad, USA) with SYBR Select Master Mix (Invitrogen). Cycling conditions were as follows: pre-denaturation for 2 min at 95°C, a 2-step reaction (40 cycles) of 10 s at 95°C and 40 s at 60°C followed by dissociation peak analysis. The sequences for oligonucleotide primers used are listed in Supplementary Table S2. The mRNA expression values of target genes were calculated with Bio-Rad CFX Manager Software. Normalization using two endogenous control genes, *ACTB* and *HPRT1*, was applied for analysis of mRNA expression values.

Ectopic expression of *TNNC1*

The coding regions of *TNNC1* was amplified by PCR and cloned into the LZRS retroviral vector plasmid with V5 epitope tag at the C-terminus along with IRES-GFP (internal ribosome entry site-green fluorescent protein) as previously described (Jung et al., 2015a; Kim et al., 2003). The control virus expresses just GFP. Preparation of high titer virus was carried out using 293GPG cells following previously published proto-

cols with minor modifications (Jung et al., 2015a; Kim et al., 2003). Detailed procedures on construction of pLZRS vectors and production of pseudotyped viral particles are available upon request.

Soft agar colony formation assay

Soft agar colony formation assay was carried out as described previously with minor modifications (Jung et al., 2015a; 2015b). NIH3T3 cells were seeded at a density of 3×10^4 per well in 12-well tissue culture plates and infected with the retrovirus. After two days, 2,000 cells were resuspended in complete media containing 0.35% Difco Noble agar (BD Biosciences, USA) and plated on the top of solidified 0.9% base agar containing complete media. Twenty-one days after plating the cells in soft agar, cells were stained with 1 mg/ml of MTT solution overnight. The colonies were counted using OpenCFU (Geissmann, 2013) version 3.9.

Conventional RT-PCR analysis

For conventional reverse transcription PCR (RT-PCR) analysis, cDNA was amplified using Platinum *Taq* DNA polymerase (Invitrogen) and primers for *TNNC1* in reaction of 30 cycles at annealing temperature of 60°C. *ACTB* expression was used as an internal control.

Colony formation assays

A549 and H2009 cells were plated at a density of 2×10^4 and 3×10^4, respectively in 12-well tissue culture plates. After incubation for 24 h, cells were infected with the retrovirus. Two days after infection, 1,000 live A549 cells and 2,000 live H2009 cells were re-plated in 6-well tissue culture plates in duplicates. Nine days (A549) or 13 days (H2009) after incubation, colonies were stained with 0.1% Coomassie Blue in 45% methanol and 10% acetic acid solution. Colony numbers were determined using OpenCFU.

Apoptosis and cell cycle analyses by flow cytometry

For apoptosis analyses, cells were seeded and infected with the retrovirus. After 96 h, trypsinized cells were collected and washed with cold PBS and resuspended in 1× Annexin V binding buffer (BD Biosciences) at a concentration of 1×10^6 cells/ml. After staining with propidium iodide and V450 annexin V (BD Biosciences), flow cytometric analyses typically using 10,000 cells were carried out using BD LSRFortessa cell analyzer. For cell cycle analyses, cells were seeded in 6-well plates and infected with the retrovirus. After 48 h, trypsinized cells were washed with cold PBS and fixed with 70% ethanol overnight. Subsequently, cells were stained with 50 μg/ml propidium iodide (PI; Sigma, USA) in PBS containing 10 μg/ml RNase A (Sigma) and 0.1% Triton X-100 at RT for 15 min. Flow cytometry for cell cycle analysis was carried out using BD LSRFortessa cell analyzer (BD Biosciences) and the distribution of a total of 10,000 nuclei was determined using BD FACSDiva software (BD Biosciences).

Western blotting analysis

TNNC1-V5-expressing cells were harvested and lysed using RIPA buffer as described previously (Jung et al., 2015a). Primary antibodies used in immunoblot analyses are as follows: anti-V5 (Invitrogen), anti-p53 (Santa Cruz Biotechnology, USA), anti-p21 Waf1/Cip1 (Cell Signaling Technology, USA), anti-CDC25C (Cell Signaling Technology), anti-Cyclin B1 (Cell Signaling Technology), anti-α-tubulin (AbFrontier, Korea), and anti-γH2AX (Millipore, USA). Peroxidase-conjugated secondary antibodies were used for detection in combination with AbSignal Western Blotting Detection Reagent kit (Abclon, Korea) or enhanced chemiluminescence detection kit (Amersham-Pharmacia Biotech, USA) following the manufacturer's protocols.

Immunofluorescence assay

For immunofluorescence, the transduced cells were fixed in 4% paraformaldehyde, permeabilized with 0.1% Triton X-100 in PBS and blocked with 1% BSA in PBS. Cells were first stained with anti-γH2AX antibody or anti-V5, followed by Alexa Fluor 594 goat anti-mouse (Invitrogen) and DAPI (4',6-diamidino-2-phenylindole) treatment and were examined by epifluorescence microscopy.

Knockdown of *TNNC1* and cell invasion assay

Cell invasion assay was performed with BD BioCoat Matrigel Invasion Chambers (BD Bioscience) according to the manufacturer's instruction. siRNA duplexes of *TNNC1* and scrambled negative control (NC) were obtained from GE Dharmacon (USA). A549 cells at 40% confluence were transfected with 40 nM *TNNC1* siRNA using Lipofectamine RNAiMAX. After 48 h, 5×10^4 cells in serum free media were transferred to the upper chamber. After 24 h of incubation, the invading cells were fixed with 100% methanol and stained with 0.1% Coomassie blue. Three random fields were selected under the light microscope and the number of the invading cells were counted using the ImageJ software (Schneider et al., 2012).

Statistical analysis

The association between *TNNC1* RNA expression and the clinicopathological features was evaluated using chi-square test. Receiver operating characteristic (ROC) curves for death and recurrence detection were constructed and the optimal cut-off value of *TNNC1* expression was determined based on Youden index. Kaplan–Meier curves and the log-rank tests were used to analyze the overall survival (OS) and the recurrence free survival (RFS) of LUAD patients using the R survival package version 2.41-3 and GraphPad Prism 6 (GraphPad Software, USA) software. The results from *TNNC1* mRNA expression levels, colony formation, apoptosis, cell cycle and invasion assays between the different groups were evaluated by two sided Student's *t*-test. Typically, data from three independent experiments were used for statistical analyses. *P* values less than 0.05 were considered statistically significant.

RESULTS

KRAS pathway and *TNNC1* have a mutually antagonistic relationship

We analyzed RNA-seq data from tumor and matched normal samples of 102 LUAD patients, and a total of 1,533 DEGs were identified as significantly down-regulated genes in tumor tissues. Tumor suppressor candidates were isolated

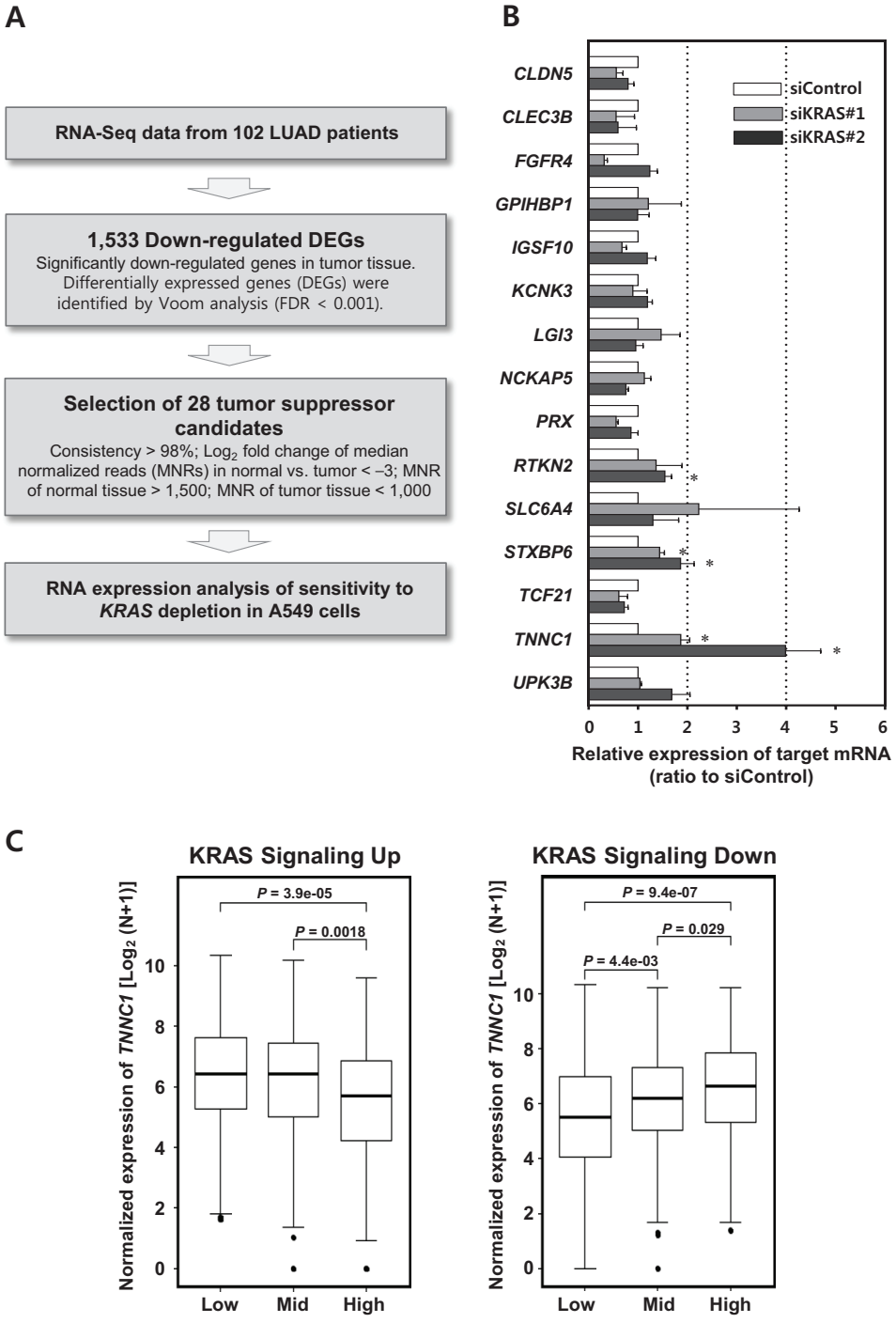

Fig. 1. Isolation of KRAS-targeted tumor suppressor candidates. (A) Schemata of the filtering pipeline for KRAS-mediated tumor suppressor candidate genes. Consistency indicates consistent direction of change for differential expression among 102 individual patients. (B) Real-time RT-PCR analyses using A549 cells transfected with two independent siRNAs specific for *KRAS*. Data are mean ± SEM of three independent experiments for each gene. Asterisk (*) represents *P* value of < 0.05 compared to the control siRNA (siControl). Note that *TNNC1* and *STXBP6* were significantly up-regulated by *KRAS* down-regulation. (C) Association of *TNNC1* RNA expression with KRAS signaling activity. For the TCGA-LUAD patients (n = 502), pathway activity was estimated from the tumor expression values (given in normalized expression level) using the GSVA algorithm for two gene sets obtained from the MSigDB (*KRAS*_Up and *KRAS*_Down). Patients were divided into high, mid, and low groups according to the pathway activity of each gene set. The middle bar in each box shows the median score. The outliers indicated by separate dots. The *TNNC1* expression levels for the two groups were shown in the box plots with two sided Student's *t*-test comparison. *P* values are indicated. Note the down-regulation of *TNNC1* in the case of high KRAS pathway activity and the opposite in the case of low KRAS pathway activity.

based on several additional filtering criteria including FDR < 0.001 in Voom analysis, consistency of > 98%, Log_2 fold change of median normalized reads (MNRs) in normal versus tumor tissue < −3, and MNRs of normal tissue > 1,500 and MNRs of tumor tissue < 1,000 (Fig. 1A). From the 28 genes thus found, we were able to obtain reliable results from real-time PCR analyses for 15 genes indicating sufficient levels of expression in A549 cells (Fig. 1B).

We proceeded to examine changes in their expression upon inhibition of *KRAS* expression by RNA interference with two independent siRNA sequences. Two genes, *STXBP6* and *TNNC1*, showed significant increases from this initial screening (Fig. 1B) although other genes such as *SLC6A4* and *UPK3B* may merit further examination. For subsequent analyses in this study, we focused on *TNNC1*.

First, we investigated the association of *TNNC1* expression with the activity of KRAS signaling pathway. Using RNA-Seq data from 502 TCGA LUAD patients, we estimated the pathway activities using the GSVA algorithm (Hanzelmann et al., 2013) for the pathways in the MSigDB database (Liberzon et al., 2011). *TNNC1* expression showed significant negative correlation with both the KRAS signaling pathway (Fig. 1C), strongly suggesting the tumor suppressive roles of TNNC1 in LUAD patients.

We further investigated the interaction between *KRAS* and *TNNC1*. First, inhibition of *KRAS* was carried out using another lung cancer cell line, H2009 in addition to A549. *TNNC1* expression was up-regulated as the consequence in both of cell lines consistent with the generality of inhibition of TNNC1 by KRAS signaling (Fig. 2A). Next, we utilized the well-established soft agar assay using NIH3T3 cells to test if TNNC1 can inhibit anchorage independent growth induced by the oncogenic KRAS mutant (Jung et al., 2015a). Retroviruses expressing *TNNC1* and $KRAS^{G12D}$ were generated and used to infect NIH3T3 cells which were subsequently seeded and cultured in soft agar. Indeed, both the size and number of colonies decreased significantly upon co-expression of *TNNC1* in $KRAS^{G12D}$ expressing cells (Fig. 2B). This is consistent with a mutually inhibitory regulation between *KRAS* and *TNNC1* and with a potentially meaningful function of *TNNC1* as a tumor suppressor.

Down-regulation of *TNNC1* expression is correlated with poor survival

We examined the expression of *TNNC1* in our group of 102 patients and in the 58 LUAD patients with matched tumor-normal data from TCGA data in detail. Both groups showed statistically significant down-regulation of *TNNC1* in tumor tissues (Fig. 3A). We examined a subset of our patient group by conventional RT-PCR and found without exception that *TNNC1* expression was down-regulated in tumors compared to matched normal tissues (Fig. 3B). We next investigated if the lowered expression of *TNNC1* has a prognostic value using our patients whose survival data to date were available using Kaplan–Meier and ROC analyses. Both OS and recurrence-free survival showed that high expression of *TNNC1* was associated with better survival although the OS did not have the statistical significance of *P* value < 0.05 most likely due to the limited number of patients (Figs. 3C

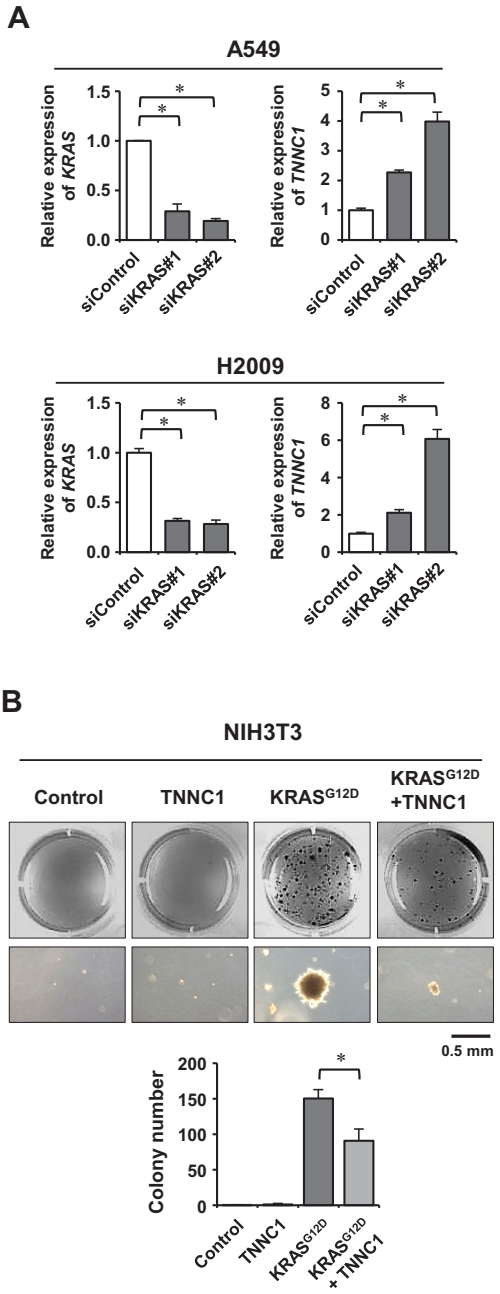

Fig. 2. Mutual inhibition of *KRAS* and *TNNC1*. (A) Real-time RT-PCR analyses using A549 and H2009 cells transfected with siRNAs specific for *KRAS*. siControl represents negative control siRNA. Data are mean ± SEM of three independent experiments. Asterisk (*) represents *P* value of < 0.05 compared to siControl. Note the down-regulation and up-regulation of *KRAS* and *TNNC1*, respectively. (B) TNNC1 inhibits $KRAS^{G12D}$-induced anchorage independent growth of NIH3T3 mouse fibroblast cells. Virus-infected cells were cultured in soft agar for 28 days and then stained with MTT solution. In the lower panels, enlarged images of representative colonies are shown. Bar graph displays colony count results from soft agar assay. Data are mean ± SEM of three independent experiments. Asterisk (*) represents *P* value of < 0.05. Note the significant decrease in both the size and number of colonies upon expression of *TNNC1*.

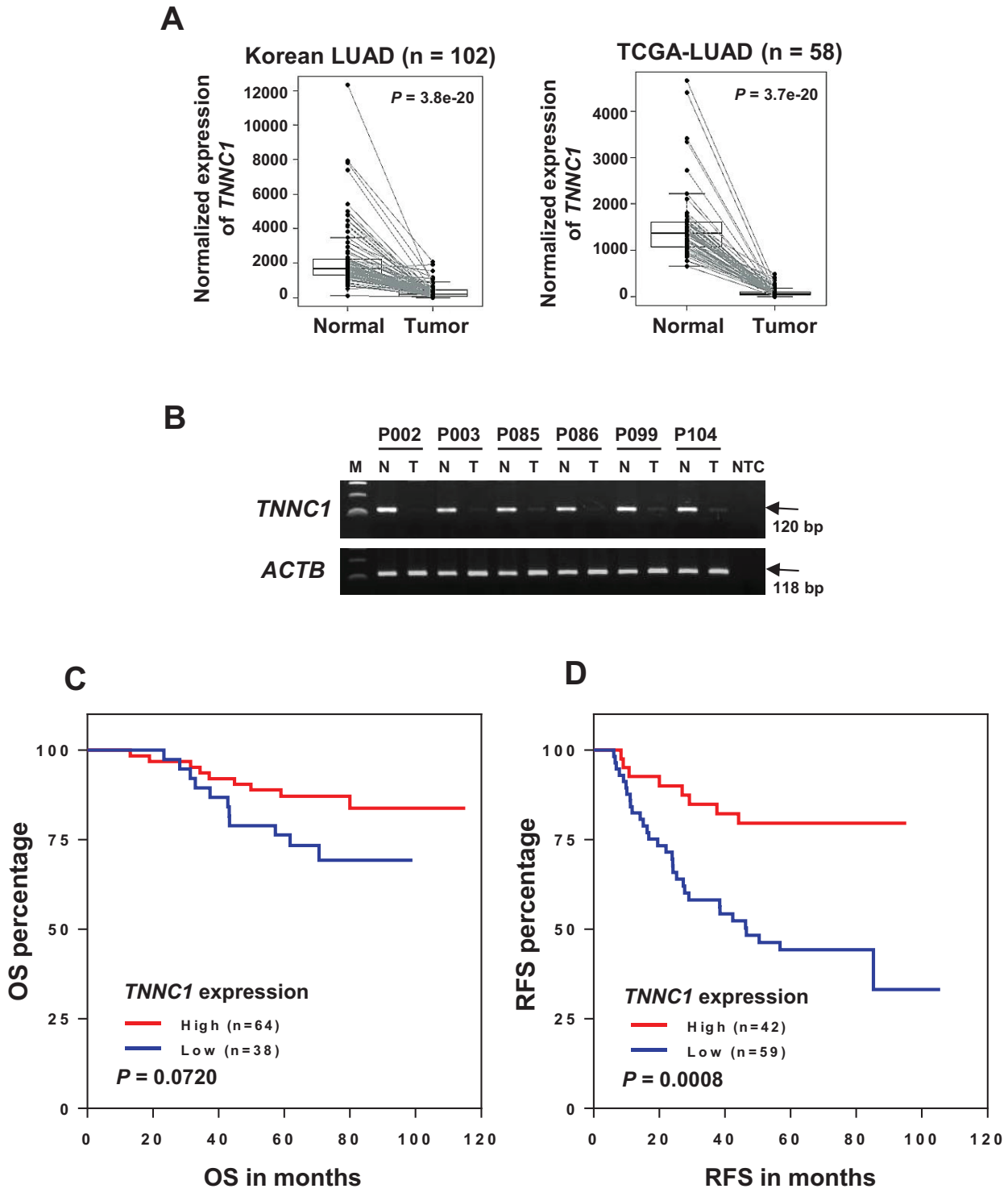

Fig. 3. Down-regulation of *TNNC1* in LUADs. (A) Box-plots of *TNNC1* RNA expression in normal-tumor matched 102 LUAD patients in this study (left panel) and of normal-tumor matched 58 LUAD patients from TCGA data (right panel). The bold line in the middle of each box represents the median level. (B) Conventional RT-PCR confirmation using normal (N) and tumor (T) tissue samples from 6 representative LUAD patients. *ACTB* was used as the amplification control. NTC stands for no template control and M stands for size markers. Tumor tissues are marked by decreased *TNNC1* expression. (C) Kaplan–Meier survival curves. LUAD patients (n = 102) were divided into two groups based on *TNNC1* RNA expression, and the survival data from high and low groups determined from ROC analysis were used for Kaplan-Meier analysis. Long-term survival was weakly co-related with the higher expression of *TNNC1*. (D) Recurrence free survival from the high and low groups showed a significant correlation with *TNNC1* transcriptional level.

and 3D). Similar analysis for the TCGA LUAD cohort using *TNNC1* expression in tumor tissue indicated that only OS was significant (P = 0.011) (Supplementary Fig. S1). The better survival for high expression group for > 5 year period is once again consistent with a meaningful role of *TNNC1* as a tumor suppressor.

TNNC1 affects cell cycle and survival

Using colony formation assay, we examined if TNNC1 has an inhibitory effect on cell growth in two independent cell

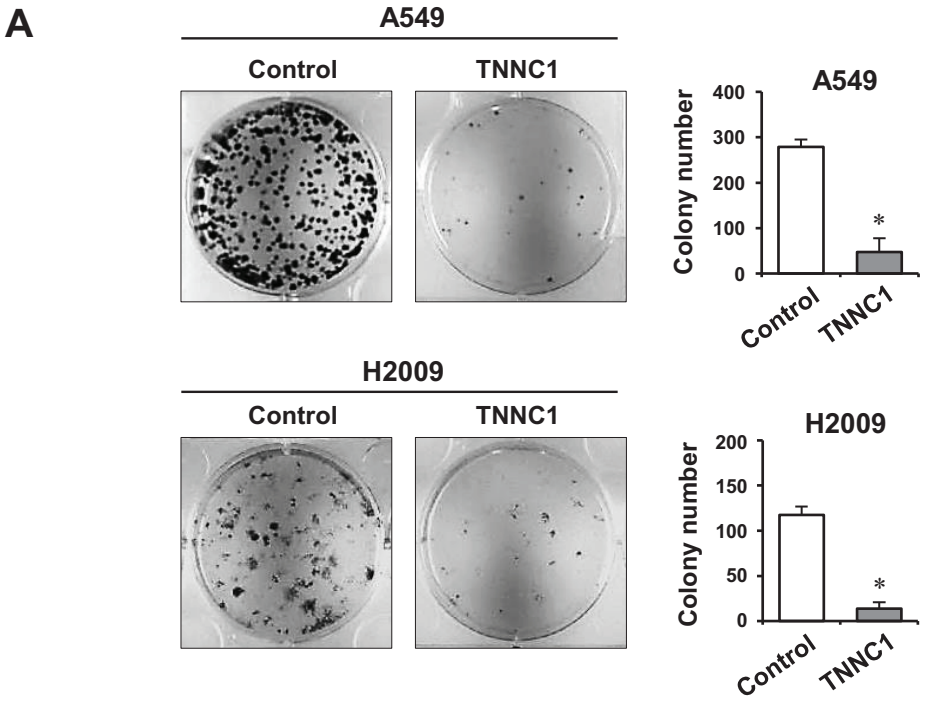

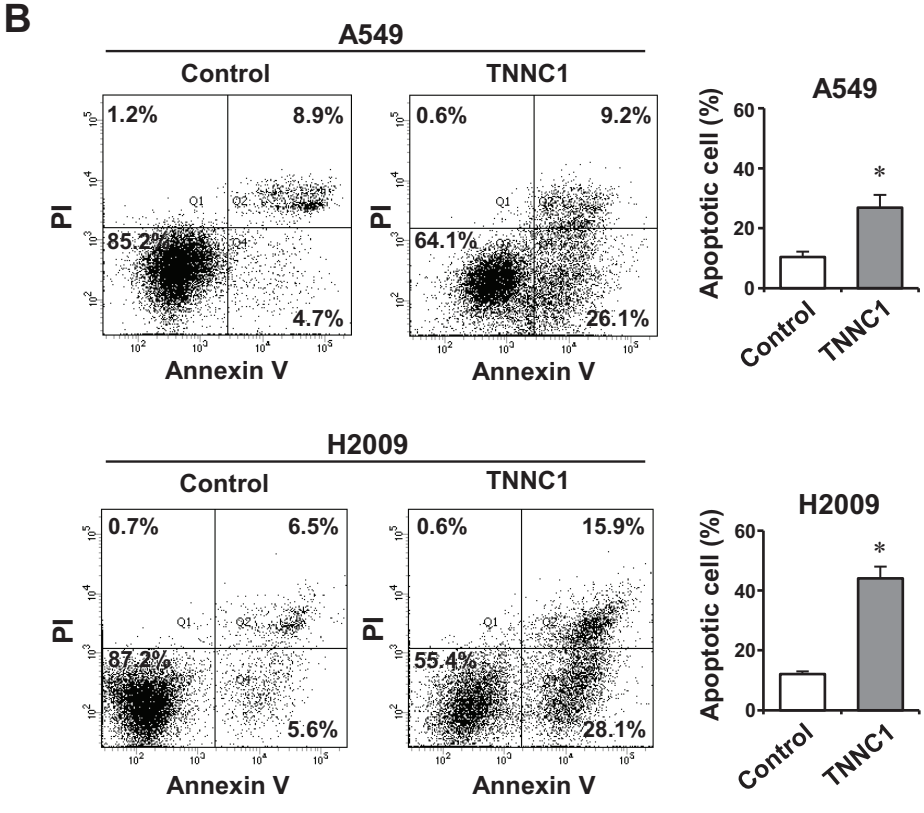

Fig. 4. Growth inhibition and apoptosis induction by *TNNC1*. (A) A549 and H2009 cells were infected with control virus or *TNNC1*-expressing virus, incubated for 9 and 13 days respectively, and resulting colonies were stained with Coomassie blue and counted. Note the strong decrease in colony numbers with *TNNC1* expression. Data are mean ± SEM of three independent experiments, and asterisk (*) represents P value of < 0.05. (B) Four days after infection of A549 and H2009 cells, apoptosis was evaluated by flow cytometric analysis after staining for PI and Annexin V. Note the strong induction of apoptosis in both A549 and H2009 cells. Graphs to the right show the results from three independent experiments as mean ± SEM. Asterisk (*) represents P value of < 0.05.

lines, A549 and H2009. Upon ectopic expression of *TNNC1*, we saw a dramatic decrease in colony numbers in both cell lines (Fig. 4A). Next, in order to determine if *TNNC1* induced apoptosis, we carried out flow cytometric analyses. Indeed, in 4 days after ectopic expression of *TNNC1*, significant increases in Annexin V and PI positive cells were seen from both A549 and H2009 cells (Fig. 4B).

One frequently seen effect of tumor suppressor expression is the induction of cell cycle arrest. We examined the cell cycle progression of A549 and H2009 cells after ectopic expression of *TNNC1* using PI staining and flow cytometric analyses. Interestingly, in 2 days after viral transduction, A549 cells showed a significant decrease in the fraction of cells in the S phase and a corresponding increase in the fraction of cells in G1 phase (Fig. 5A). This was consistent with G1 arrest induction. In contrast, H2009 cells showed increase in S and

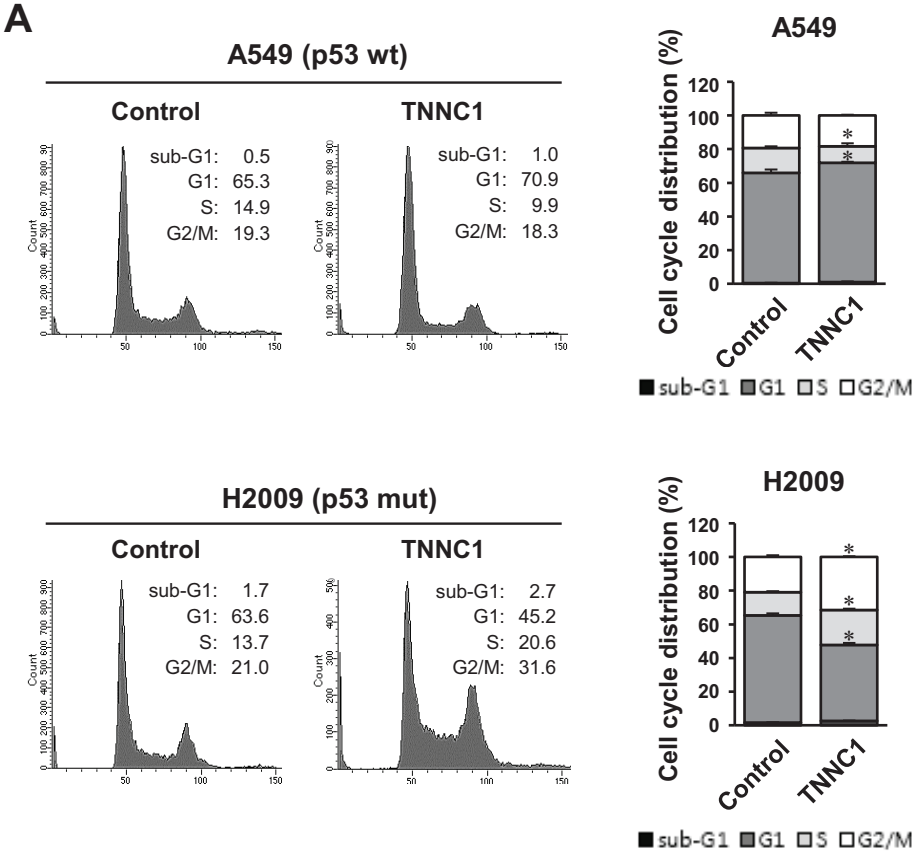

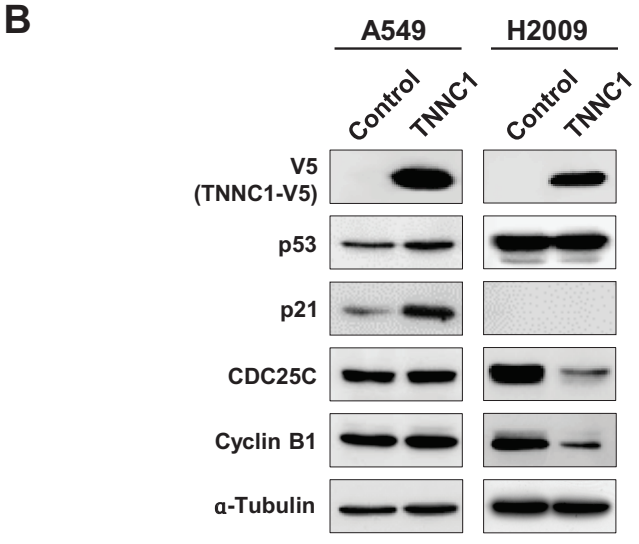

Fig. 5. Cell cycle arrest induced by *TNNC1*. Ectopic expression of *TNNC1* induces cell cycle arrest at different stages depending on p53 mutation status. (A) A549 and H2009 cells were infected with control virus or *TNNC1*-expressing virus, and cell cycle progression was analyzed by flow cytometry after 2 days. Representative histograms are shown. Graphs to the right show the proportion of cells in each cell cycle phase from flow cytometric analyses. Note that in A549 cells with the wild type p53, G1 arrest is induced. In H2009 cells with mutant p53, S and G2/M arrest is induced. Data are mean ± SEM of three independent experiments. Asterisk (*) represents *P* value of < 0.05. (B) Immunoblot analyses of A549 and H2009 cell lysates after 2 days of viral infection. α-Tubulin was used as the loading control. Note the induction of p53 and p21 in A549 cells and the reduction of CDC25C and Cyclin B1 in H2009 cells.

G2/M phase cells and decrease in G1 phase (Fig. 5A) consistent with G2/M arrest. The respective arrest patterns were corroborated by immunoblotting for cell cycle protein markers. Specifically, in A549 cells, p53 and p21 are up-regulated while CDC25C and Cyclin B1 were not altered (Fig. 5B). In H2009 cells, p53 expression was not altered while expression of CDC25C and Cyclin B1 decreased (Fig. 5B). The differential effects on cell cycle most likely reflect the mutation status of p53. It has been reported in multiple studies that with wild type p53 as in the case of A549 cells, cell cycle is arrested by a serial action of p53 and p21 at the G1 phase. In cells without intact p53 as in H2009 cells, the cell cycle bypasses G1 checkpoint and the arrest occurs later in G2/M stage (Hata et al., 2005; Ma et al., 2017; Normand et al., 2005). Interestingly, p21 expression is not seen in H2009 cells possibly reflecting the induction of this gene by p53 which is inactive in H2009 cells (Abbas and Dutta, 2009).

The differential response based on p53 status suggested that TNNC1 possibly induces or mediates DNA damage response which would in turn normally induce p53 response and G1 arrest. We examined cells after ectopic expression of *TNNC1* for DNA damage response whose hallmark is accumulation of γH2AX, the phosphorylated form of H2AX signifying double-strand breaks. Indeed, within 24 h after introduction of *TNNC1*, induction of γH2AX was detected by immunoblotting and by immunocytochemical staining in both A549 (Fig. 6, upper panels) and H2009 cells (Fig. 6, lower panels). We examined the expression pattern of TNNC1 in the cell using the epitope tag and found that it is expressed mostly in the nucleus (Supplementary Fig. S2) suggesting a

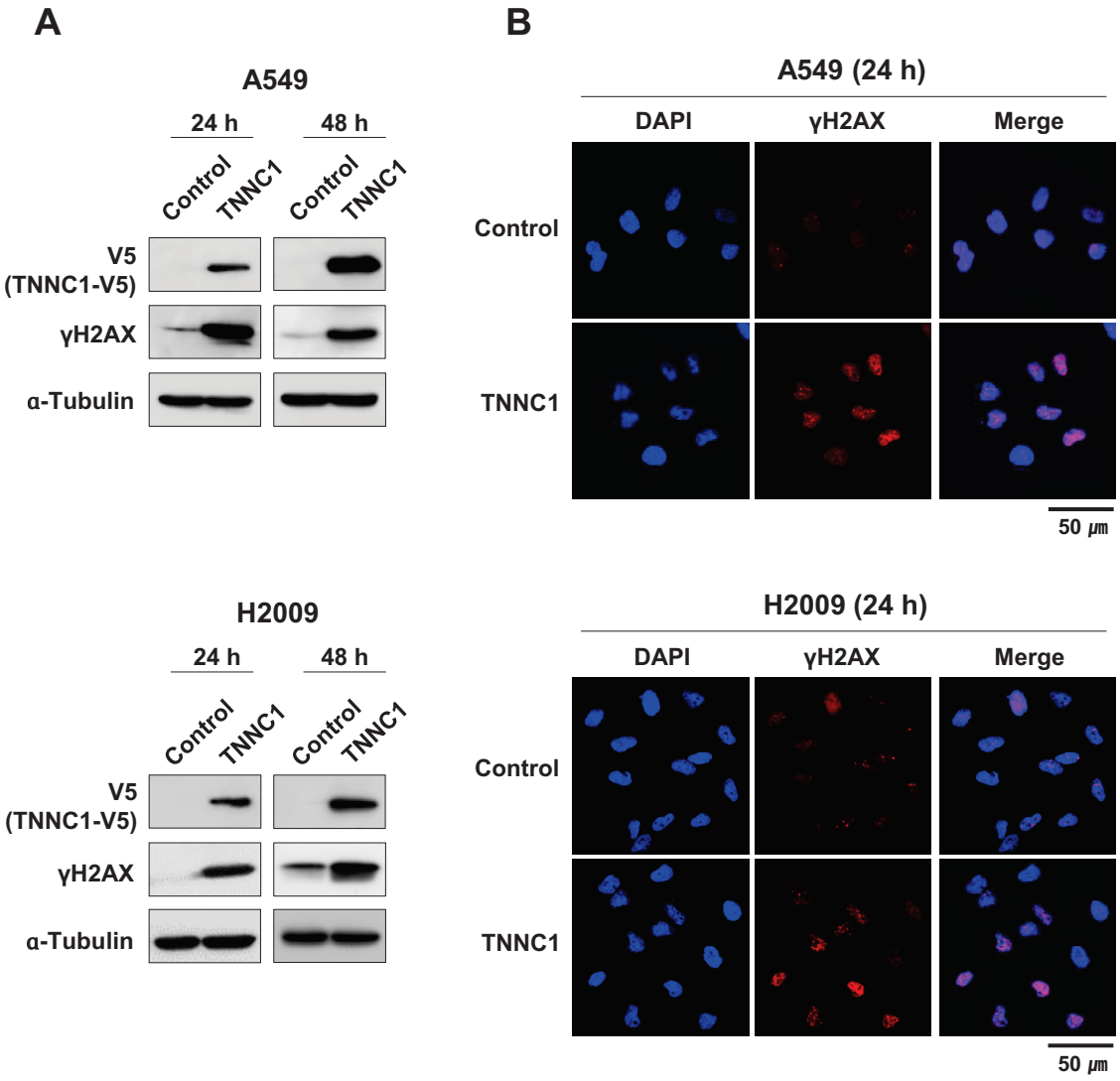

Fig. 6. DNA damage response induced by *TNNC1*. A549 and H2009 cells were infected with control virus or *TNNC1*-expressing virus and induction of γH2AX was analyzed. (A) Immunoblot analyses of γH2AX in A549 and H2009 cells. Note the strong γH2AX-induction upon expression of *TNNC1* in 24 h. α-Tubulin was used as the loading control. (B) Immunofluorescence analysis of γH2AX in A549 and H2009 cells. DAPI counter-stained nuclei are positive for γH2AX in 24 h.

Table 1. Association of *TNNC1* expression and clinical features in 102 lung adenocarcinoma patients

Clinicopathological features		*TNNC1* expression		χ^2	*P* value
		Low (n = 38)	High (n = 64)		
Age (y)	< 62	19	31	0.02	0.879
	≥ 62	19	33		
Tumor size (cm)	< 3	21	47	6.52	0.038*
	3-5	16	12		
	≥ 5	1	4		
	Null	0	1		
Pathologic stage[a]	1	23	41	1.89	0.595
	2	8	8		
	3	7	14		
	4	0	1		
T stage[a]	1	15	41	13.2	0.004*
	2	23	17		
	3	0	5		
	4	0	1		
N stage[a]	0	24	44	4.7	0.094
	1	7	3		
	2	7	14		
	Null	0	3		
Differentiation grade	Well differentiated	1	8	2.7	0.257
	Moderately differentiated	29	47		
	Poorly differentiated	3	4		
	Null	5	5		
Vascular invasion	No	33	61	6.9	0.009*
	Yes	4	0		
	Null	1	3		
Lymphatic invasion	No	21	44	2.4	0.118
	Yes	16	17		
	Null	1	3		
Visceral pleural invasion	No	21	53	8.1	0.004*
	Yes	15	10		
	Null	2	1		
Recurrence status	No	21	41	1	0.326
	Yes	17	22		
	Null	0	1		

Major clinicopathological features and subcategories therein are listed. Patients are grouped into either high or low *TNNC1* expression groups as in Fig. 3C. The chi-squared test shows significant correlation with tumor size, tumor stage, vascular invasion, and visceral pleural invasion.
Null, no data.
$*P < 0.05$.
[a]The clinical and pathological stage was determined according to the 7th edition of the American Joint Committee on Cancer.

possibly direct and physical role of TNNC1 in inducing DNA damage response. Taken together, the progression of events is consistent with induction of DNA damage followed by cell cycle arrest ultimately leading to apoptosis.

Down-regulation of *TNNC1* enhances invasiveness of tumor

We next used clinical data to test if any of the major clinical parameters were correlated with the expression level of *TNNC1* (Table 1). We used the two patient groups, high *TNNC1* expression group (n = 64) and low *TNNC1* expression group (n = 38), defined from the OS analysis and performed Pearson's chi-squared test and examined for statistical significance. Interestingly, in addition to tumor size and tumor stage, two additional parameters, vascular invasion and visceral pleural invasion showed *P* value of 0.009 and 0.004 consistent with that higher the *TNNC1* expression, less likely for invasion to have happened. We attempted to confirm this correlation using Matrigel invasion assay. While ectopic expression of *TNNC1* had little effect on the behavior of A549 cells (data not shown), knockdown of *TNNC1* by specific siRNAs promoted invasive activity of the cells over 2 fold (Fig. 7, Supplementary Fig. S3) suggesting that down-regulation of *TNNC1* may be causally associated with invasiveness in LUAD.

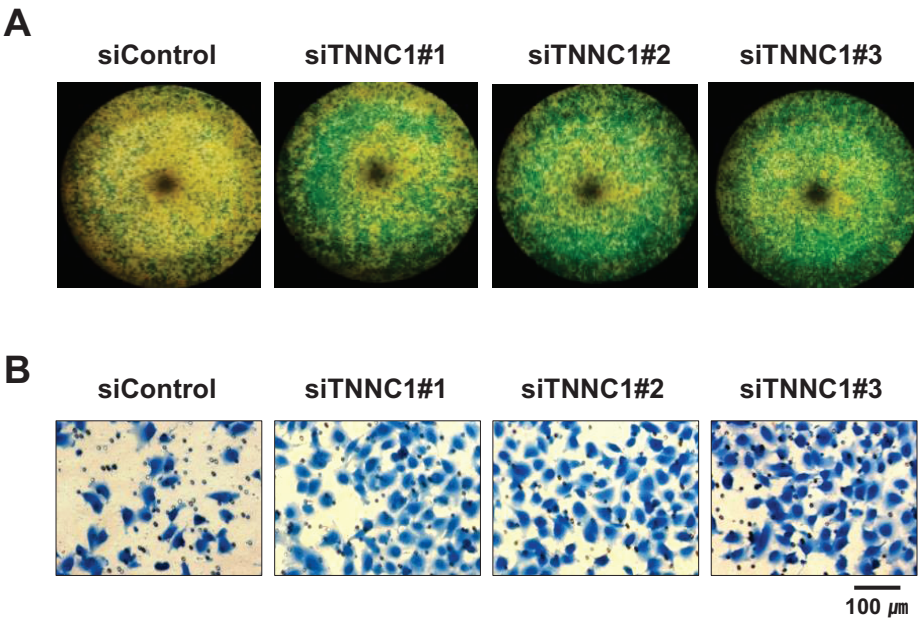

Fig. 7. TNNC1-mediated cell invasion. A549 cells were transfected with either siControl or one of the three independent siRNAs specifically targeting *TNNC1*. Transfected cells were used for matrigel invasion assay. Typical results are shown at low (A) and high (B) magnification after Coomassie blue staining. (C) Quantification of transwell migration assays by *TNNC1* knockdown. The graph shows results from three independent assays. Bars represent as mean ± SEM and asterisk (*) represents *P* value of < 0.05.

DISCUSSION

Multiple large-scale high throughput sequencing projects for diverse types of cancers have been reported recently. In the case of lung cancer, a comprehensive multi-layered profiling of 230 LUAD is the most representative (Cancer Genome Atlas Research Network, 2014). While numerous mutations, DEGs and altered pathways have been proposed for their potential involvement, each event clearly needs to be carefully re-examined for its significance in carcinogenesis by experimental validation as a large fraction of them is likely to be the so-called 'passenger' events.

Several studies have reported that various troponin genes are expressed in a variety of non-contracting cells and involved in cancer development although the exact function and mechanism for their activities are barely known (Johnston et al., 2018). From our sequencing analyses of matched normal and tumor samples of over 100 never-smoker female patients of LUAD, *TNNC1* was identified as a down-regulated DEG, and multiple lines of evidence from our molecular analyses on cell growth, cell cycle alteration, DNA damage and apoptosis indicate that *TNNC1* indeed functions as a tumor suppressor. It appears that DNA damage was the first event to take place after ectopic expression of *TNNC1*. How exactly DNA damage response was induced is not clear, but the effect may be direct as TNNC1 has been reported to be localized in the nucleus in cancer cells (Casas-Tinto et al., 2016; Johnston et al., 2018; Sahota et al., 2009). The ectopic protein used in this study is also found in nucleus consistent with such reports (Supplementary Fig. S2). One caveat is that we were not able to find a commercial antibody that consistently reflects the ectopic expression or inhibition by RNA interference of the target gene, *TNNC1*.

Our data indicate that *TNNC1* has a potential prognostic

value for LUAD as down-regulation is highly correlated with invasiveness of the cancer and with decreased likelihood of recurrence-free survival. Of note, visceral pleural invasion is a major indicator for aggressiveness for non-small cell lung cancer which encompasses LUAD (Brewer, 1977; Shimizu et al., 2005). Down-regulation of *TNNC1* in fact enhanced invasiveness of A549 cells *in vitro*, and this should provide a setting for studying detailed molecular mechanisms for this function of *TNNC1* down the road.

It is also interesting that *TNNC1* is targeted for down-regulation by KRAS signaling pathway. Furthermore, TNNC1 was shown to inhibit KRAS activity as shown in anchorage independent growth of NIH3T3 cells. The data, although limited by the use of a fibroblast cell line rather than LUAD cell lines, are consistent with that down-regulation of *TNNC1* may be a necessary step for efficient oncogenesis mediated by activation of KRAS pathway or mutation of component genes. Given that mutations in *EGFR*, *KRAS* and *BRAF* collectively account for up to 40% of the LUAD, finding targets or regulators of this pathway seems to be of particular importance (Brainard and Farver, 2019; Pao and Girard, 2011).

Although our data together render *TNNC1* as a prime tumor suppressor candidate for LUAD, the gene is not likely to be a universal tumor suppressor. Of the 17 types of tumor with sufficient cases of matched tumor and normal tissues, 6 types including LUAD, HNSC, KICH, KIRC, KIRP and LUSC show significant down-regulation ($P < 0.05$) in tumor tissues while for LIHC, STAD, and UCEC, the opposite appears to be the case (Supplementary Fig. S4; HNSC, head and neck squamous cell carcinoma; KICH, kidney chromophobe; KIRC, kidney renal clear cell carcinoma; KIRP, kidney renal papillary cell carcinoma; LUSC, lung squamous cell carcinoma; LIHC, liver hepatocellular carcinoma; STAD, stomach adenocarcinoma; UCEC, uterine corpus endometrial carcinoma). Examination of survival in these cancers indicates that only in STAD the expression level of *TNNC1* is correlated with survival (Supplementary Fig. S5). *TNNC1* could therefore function as an oncogene in STAD. An outstanding question thus would be if the same molecular activity of *TNNC1* may be oncogenic in certain cellular context. Other remaining questions include whether *TNNC1* functions as a tumor suppressor in a manner that requires formation of the troponin complex. More likely, it may be that *TNNC1* is truly a 'moon-lighting' protein with a novel mode of action in functioning as a tumor suppressor as we saw virtually no expression of Troponin I and Troponin T at least at the mRNA level.

Note: Supplementary information is available on the Molecules and Cells website (www.molcells.org).

ACKNOWLEDGMENTS

Authors thank all members of Ewha Research Center for Systems Biology for the helpful discussions. This research was supported by funding from the Ministry of Science and ICT via National Research Foundation, Republic of Korea (NRF-2015K1A4A3047851).

AUTHOR CONTRIBUTIONS

S.K., Jaewon K., Yeonjoo J., and Yukyung J. performed experiments and analyzed data. Yeonwha J., H.Y.L., and Juhee K. provided technical support and performed experiments. B.J.P. and J.L. prepared and provided samples and reagents. Jhingook K., S.L., and Jaesang K. conceived the study and wrote the manuscript.

CONFLICT OF INTEREST

The authors have no potential conflicts of interest to disclose.

ORCID

Suyeon Kim https://orcid.org/0000-0001-9338-3132
Jaewon Kim https://orcid.org/0000-0003-3418-4875
Yeonjoo Jung https://orcid.org/0000-0002-3096-0091
Yukyung Jun https://orcid.org/0000-0002-4025-7164
Yeonhwa Jung https://orcid.org/0000-0001-8878-9074
Hee-Young Lee https://orcid.org/0000-0002-7618-6951
Juhee Keum https://orcid.org/0000-0001-9546-8041
Byung Jo Park https://orcid.org/0000-0001-5217-4764
Jinseon Lee https://orcid.org/0000-0003-3042-6697
Jhingook Kim https://orcid.org/0000-0002-3828-0453
Sanghyuk Lee https://orcid.org/0000-0001-9230-7461
Jaesang Kim https://orcid.org/0000-0002-7659-4242

REFERENCES

Abbas, T. and Dutta, A. (2009). p21 in cancer: intricate networks and multiple activities. Nat. Rev. Cancer *9,* 400-414.

Berezowsky, C. and Bag, J. (1992). Slow troponin C is present in both muscle and nonmuscle cells. Biochem. Cell Biol. *70,* 691-697.

Brainard, J. and Farver, C. (2019). The diagnosis of non-small cell lung cancer in the molecular era. Mod. Pathol. *32*(Suppl 1)*,* 16-26.

Brewer, L.A. (1977). Patterns of survival in lung cancer. Chest *71,* 644-650.

Cancer Genome Atlas Research Network (2014). Comprehensive molecular profiling of lung adenocarcinoma. Nature *511,* 543-550.

Casas-Tinto, S., Maraver, A., Serrano, M., and Ferrus, A. (2016). Troponin-I enhances and is required for oncogenic overgrowth. Oncotarget *7,* 52631-52642.

Cerami, E., Gao, J., Dogrusoz, U., Gross, B.E., Sumer, S.O., Aksoy, B.A., Jacobsen, A., Byrne, C.J., Heuer, M.L., Larsson, E., et al. (2012). The cBio cancer genomics portal: an open platform for exploring multidimensional cancer genomics data. Cancer Discov. *2,* 401-404.

Chase, P.B., Szczypinski, M.P., and Soto, E.P. (2013). Nuclear tropomyosin and troponin in striated muscle: new roles in a new locale? J. Muscle. Res. Cell Motil. *34,* 275-284.

Chen, C., Liu, J.B., Bian, Z.P., Xu, J.D., Wu, H.F., Gu, C.R., Shi, Y., Zhang, J.N., Chen, X.J., and Yang, D. (2014). Cardiac troponin I is abnormally expressed in non-small cell lung cancer tissues and human cancer cells. Int. J. Clin. Exp. Pathol. *7,* 1314-1324.

Gao, J., Aksoy, B.A., Dogrusoz, U., Dresdner, G., Gross, B., Sumer, S.O., Sun, Y., Jacobsen, A., Sinha, R., Larsson, E., et al. (2013). Integrative analysis of complex cancer genomics and clinical profiles using the cBioPortal. Sci. Signal. *6,* pl1.

Geissmann, Q. (2013). OpenCFU, a new free and open-source software to count cell colonies and other circular objects. PLoS One *8,* e54072.

Hanzelmann, S., Castelo, R., and Guinney, J. (2013). GSVA: gene set variation analysis for microarray and RNA-seq data. BMC Bioinformatics *14,* 7.

Hata, T., Yamamoto, H., Ngan, C.Y., Koi, M., Takagi, A., Damdinsuren, B., Yasui, M., Fujie, Y., Matsuzaki, T., Hemmi, H., et al. (2005). Role of p21waf1/cip1 in effects of oxaliplatin in colorectal cancer cells. Mol. Cancer Ther. *4,*

1585-1594.

Johnston, J.R., Chase, P.B., and Pinto, J.R. (2018). Troponin through the looking-glass: emerging roles beyond regulation of striated muscle contraction. Oncotarget *9,* 1461-1482.

Jung, Y., Jun, Y., Lee, H.Y., Kim, S., Keum, J., Lee, Y.S., Cho, Y.B., Lee, S., and Kim, J. (2015a). Characterization of SLC22A18 as a tumor suppressor and novel biomarker in colorectal cancer. Oncotarget *6,* 25368-25380.

Jung, Y., Yong, S., Kim, P., Lee, H.Y., Keum, J., Lee, S., and Kim, J. (2015b). VAMP2-NRG1 fusion gene is a novel oncogenic driver of non-small-cell lung adenocarcinoma. J. Thorac. Oncol. *10,* 1107-1111.

Kim, J., Lo, L., Dormand, E., and Anderson, D.J. (2003). SOX10 maintains multipotency and inhibits neuronal differentiation of neural crest stem cells. Neuron *38,* 17-31.

Law, C.W., Chen, Y., Shi, W., and Smyth, G.K. (2014). Voom: precision weights unlock linear model analysis tools for RNA-seq read counts. Genome Biol. *15,* R29.

Leung, C.S., Yeung, T.L., Yip, K.P., Pradeep, S., Balasubramanian, L., Liu, J., Wong, K.K., Mangala, L.S., Armaiz-Pena, G.N., Lopez-Berestein, G., et al. (2014). Calcium-dependent FAK/CREB/TNNC1 signalling mediates the effect of stromal MFAP5 on ovarian cancer metastatic potential. Nat. Commun. *5,* 5092.

Li, B. and Dewey, C.N. (2011). RSEM: accurate transcript quantification from RNA-Seq data with or without a reference genome. BMC Bioinformatics *12,* 323.

Liberzon, A., Subramanian, A., Pinchback, R., Thorvaldsdottir, H., Tamayo, P., and Mesirov, J.P. (2011). Molecular signatures database (MSigDB) 3.0. Bioinformatics *27,* 1739-1740.

Ma, Y., Silveri, L., LaCava, J., and Dokudovskaya, S. (2017). Tumor suppressor NPRL2 induces ROS production and DNA damage response. Sci. Rep. *7,* 15311.

Moses, M.A., Wiederschain, D., Wu, I., Fernandez, C.A., Ghazizadeh, V., Lane, W.S., Flynn, E., Sytkowski, A., Tao, T., and Langer, R. (1999). Troponin I is present in human cartilage and inhibits angiogenesis. Proc. Natl. Acad. Sci. U. S. A. *96,* 2645-2650.

Normand, G., Hemmati, P.G., Verdoodt, B., von Haefen, C., Wendt, J., Guner, D., May, E., Dorken, B., and Daniel, P.T. (2005). p14ARF induces G2 cell cycle arrest in p53- and p21-deficient cells by down-regulating p34cdc2 kinase activity. J. Biol. Chem. *280,* 7118-7130.

Pao, W. and Girard, N. (2011). New driver mutations in non-small-cell lung cancer. Lancet Oncol. *12,* 175-180.

Sahota, V.K., Grau, B.F., Mansilla, A., and Ferrus, A. (2009). Troponin I and Tropomyosin regulate chromosomal stability and cell polarity. J. Cell Sci. *122*(Pt 15), 2623-2631.

Schmidt, K., Hoffend, J., Altmann, A., Kiessling, F., Strauss, L., Koczan, D., Mier, W., Eisenhut, M., Kinscherf, R., and Haberkorn, U. (2006). Troponin I overexpression inhibits tumor growth, perfusion, and vascularization of morris hepatoma. J. Nucl. Med. *47,* 1506-1514.

Schneider, C.A., Rasband, W.S., and Eliceiri, K.W. (2012). NIH Image to ImageJ: 25 years of image analysis. Nat. Methods *9,* 671-675.

Shimizu, K., Yoshida, J., Nagai, K., Nishimura, M., Ishii, G., Morishita, Y., and Nishiwaki, Y. (2005). Visceral pleural invasion is an invasive and aggressive indicator of non-small cell lung cancer. J. Thorac. Cardiovasc. Surg. *130,* 160-165.

Siegel, R.L., Miller, K.D., and Jemal, A. (2018). Cancer statistics, 2018. CA Cancer J. Clin. *68,* 7-30.

Wang, K., Singh, D., Zeng, Z., Coleman, S.J., Huang, Y., Savich, G.L., He, X., Mieczkowski, P., Grimm, S.A., Perou, C.M., et al. (2010). MapSplice: accurate mapping of RNA-seq reads for splice junction discovery. Nucleic. Acids. Res. *38,* e178.

Yu, N., Yong, S., Kim, H.K., Choi, Y.L., Jung, Y., Kim, D., Seo, J., Lee, Y.E., Baek, D., Lee, J., et al. (2019). Identification of tumor suppressor miRNAs by integrative miRNA and mRNA sequencing of matched tumor-normal samples in lung adenocarcinoma. Mol. Oncol. *13,* 1356-1368.